photonics

MDPI

Communication

Dynamic Tunable Meta-Lens Based on a Single-Layer Metal Microstructure

Xiangjun Li [1,2], Huadong Liu [1,2], Xiaomei Hou [1,2] and Dexian Yan [1,2,*]

[1] Key Laboratory of Electromagnetic Wave Information Technology and Metrology of Zhejiang Province, College of Information Engineering, China Jiliang University, Hangzhou 310018, China
[2] Center for THz Research, China Jiliang University, Hangzhou 310018, China
* Correspondence: yandexian1991@163.com

Abstract: Ultra-thin focusing meta-lenses based on the metasurface structure with adjustable focal length show important applicant value in compact systems, especially in on-chip terahertz spectroscopy, imaging systems, and communication systems. A stretchable substrate, dynamic focusing meta-lens based on the cross-polarized metal C-shaped split ring resonators (SRRs) is designed and investigated. At the operation frequency of 0.1 THz, the operation characteristics of the unit cell structure and the formed meta-lens are investigated. The phase of the unit cell structures can be modulated by changing the rotation angle, width, and symmetry axis of the C-shaped metal SRRs. When the terahertz wave is incident vertically, the focusing performance can be achieved based on the specific arrangement of the metasurface unit cells. By stretching the flexible substrate of the meta-lens, the dynamic focusing effect can be realized. When the substrate stretches from 100% to 120%, the focal length changes from 59.8 mm to 125.2 mm, the dynamic focusing range is 109.4% of the minimum focal length, and the focusing efficiency changes between 5.5% and 10.5%.

Keywords: terahertz; metasurface; flexible substrate; dynamic focusing

Citation: Li, X.; Liu, H.; Hou, X.; Yan, D. Dynamic Tunable Meta-Lens Based on a Single-Layer Metal Microstructure. *Photonics* **2022**, *9*, 917. https://doi.org/10.3390/photonics9120917

Received: 2 November 2022
Accepted: 24 November 2022
Published: 29 November 2022

1. Introduction

Terahertz waves (0.1–10 THz) are located between microwaves and infrared waves. Due to their special location they have many advantages, such as fingerprinting, living body safety, and non-polar material transmission, showing huge application potential in many fields including terahertz communications, non-destructive testing, homeland security, astronomy detection, medical diagnosis, and so on [1]. In the process of terahertz technology moving towards wide applications, high-power terahertz sources, high-sensitivity terahertz detectors, and compact and efficient terahertz functional devices are lacking. In recent years, metasurfaces based on subwavelength scatter arrays have exhibited great advantages of being ultra-flexible, ultra-thin, and light in the field of beam steering, which are expected to realize the miniaturization and integration of terahertz systems [2]. Capasso et al. designed a new type of optical static metasurfaces, and established the generalized Snell's law, which strongly promoted the study of metasurfaces [3]. However, in many practical applications, static metasurface structures cannot dynamically modulate terahertz waves in real time. At present, there are two main methods for the regulation of dynamic metasurfaces [4]. One method is to change the material properties of the metasurface unit cell to realize the tunable metasurfaces based on electric, magnetic, thermal, light, and other excitation [5–9]. Generally, functional materials, including graphene, VO2, GST, liquid crystal, and so on, are treated to realize the switchable metasurfaces. The other method is based on the dynamic change in the geometric parameters of metasurface structures. In this case, the dielectric elastomer actuator (DEA) [10–12], micro-electro-mechanical system (MEMS) [13–15], microfluidics [16], soft-matter [17], liquid crystal [18], and mechanics [19] are used to realize the reconfigurable metasurfaces.

Geometric structure dynamically reconfigurable metasurfaces adjust unit cell structure and unit cell space through mechanical deformation. The dynamic modulation of metasurface unit cell structures is achieved in the microwave region by treating microfluidic and liquid metals [20], which are difficult to realize in higher frequency regions due to limitations of machining accuracy and microfluidic drag constraints. The metasurfaces based on polydimethylsiloxane (PDMS) flexible substrates can adjust the distance between the unit cells by treating MEMS or EDA, which are widely used in the broad band electromagnetic spectrum from microwave to optical frequency. Based on this operation mechanism, a variety of functional devices including beam control [20], dynamic polarization conversion [21], and tunable meta-lenses are implemented [22,23]. Ee et al. embed metal strip-like microstructures into PDMS substrates to realize a flexible and stretchable zoom meta-lens in the optical band, with a stretching range of 130% and a wide dynamic focusing range [22]. Kamali et al. encapsulated the metasurface of subwavelength silicon nanopillars in PDMS in the near-infrared band, with a stretching range of 150% and a dynamic focusing range of 130% [24]. In addition, in 2018, Callewaert et al. used 3D-printing technology to prepare a millimeter-wavelength (36 GHz), stretchable, all-media focusing meta-lens [23], which can achieve 4x focusing with a stretching coefficient of only 75%. However, terahertz dynamic focusing metasurfaces based on PDMS substrates are rarely studied. Our group designed a dynamic focusing graphene-based metasurface reflector based on the flexible PDMS substrate working at the frequency of 1.0 THz [25]. By changing the chemical potential and width of the graphene strips, the reflective phase covers the 0–2π. The dynamic change in the focal length of the device can be achieved by stretching the PDMS substrate.

In this paper, based on the cross-polarized metal C-shaped split ring resonator (SRR), a stretchable substrate, dynamic focusing, terahertz metal meta-lens is designed and investigated at the frequency of 0.1 THz. The unit cell structure is composed of a metal SRR and a PDMS substrate. The operation characteristics of the unit cell are analyzed. The meta-lens structure, composed of different C-shaped metal SRRs, can provide 0–2π phase variation. The dynamic focusing effect can be realized by stretching the stretchable PDMS substrate. The working performances of the dynamic focusing meta-lenses are investigated.

2. Unit Cell Design and Characteristics Analysis

In metasurface devices, subwavelength antennas are one of the main components of metasurface structures. In general, the modulation unit cell structure of electromagnetic waves usually has two or more open ports. Unit cell structures such as V-type, C-type, H-type, and L-type structures are widely used. For the same polarized scattered light, the change in the antenna geometric size and rotation angle can only reach a 0–π phase, while a phase shift of 0–2π can be achieved by applying cross-polarized scattering light.

Figure 1 depicts the unit cell structure of the C-shaped SRR transmission metasurface. As shown in Figure 1a, the unit cell structure is composed of a top C-shaped metal SRR and PDMS substrate. PDMS is a kind of polymer with a refractive index of 1.53 in the terahertz band [26]. C-shaped metal SRR can be constructed on PDMS with silver nanowire by pre-strained technology [27]. PDMS substrate is fixed on the two-dimensional stretching equipment with a stretching factor of 120% in the x-direction and is kept fixed in the y-axis direction. Then, the metallic nano-wire ink is printed onto the substrate using a piezoelectric inkjet printer. The manufacturing process ensures the conductivity of SRRs during the stretching process. This kind of material provides the advantages of easy processing, simple preparation, good stretchable properties, and so on. Figure 1b depicts the detailed structural features of the C-shaped metal SRR. The period of the unit cell structure is p = 1600 μm which is much smaller than the wavelength of 0.1 THz, and the thickness of the substrate is d = 500 μm with a suitable stretching and toughness property. The parameters r_1, r_2, α, and θ are the geometric features of the C-shaped metal SRRs.

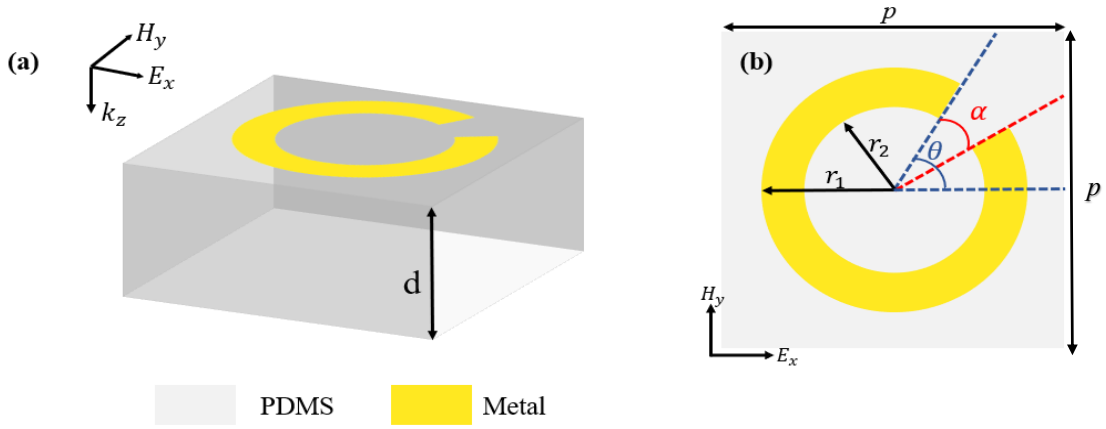

Figure 1. Unit cell structure of the C-shaped metal SRR. (**a**) Three-dimensional illustration of the unit cell structure; (**b**) top view of the unit cell structure.

Figure 2 shows the part meta-lens structure composed of different C-shaped metal SRRs. The phases of the output terahertz wave can be modulated by changing the geometrical parameters of the C-shaped metal SRRs when the period is constant. The y direction is the periodic structure, and the stretching operation is performed in the x direction. Based on the cross-polarization theory, electromagnetic waves can realize focus in the y direction along a line above the meta-lens. The diameter of the meta-lens is approximately 80 mm 50×50 unit cells.

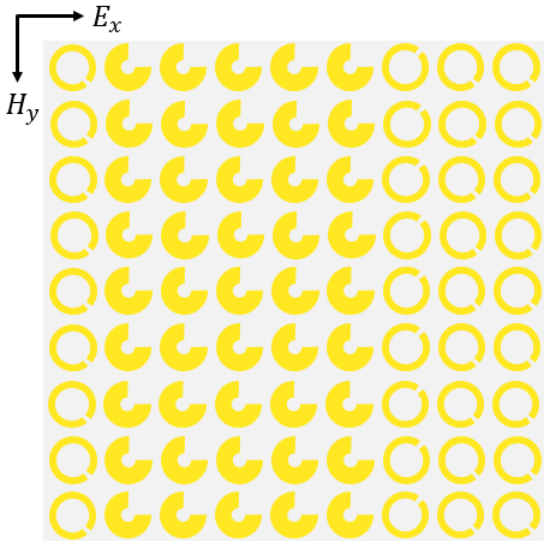

Figure 2. Schematic diagram of the part single-layer metal meta-lens in the x–y plane.

The phase distribution corresponding to different positions along the x direction of the designed dynamic adjustable meta-lens satisfies the expression [28]:

$$\varphi(x) = \frac{2\pi}{\lambda}\left(\sqrt{r^2 + f^2} - f\right) \quad (1)$$

where f = 60 mm is the initial focal length, λ = 3 mm is the wavelength of the incident wave related to the working frequency of 0.1 THz, and r is the position of the discrete unit structure from the origin of the meta-lens.

The working principle of the stretchable substrate, single-layer, metal structure dynamic tunable meta-lens is shown in Figure 3. The tunable focusing property of the meta-lens is realized by the applied external strain force to stretch. Fixed the dimension

along the *y*-axis, the length of the meta-lens along the *x*-axis is stretched in the range S = 100% to S = 120% by stretching equipment. In the simulation, the stretching effect can be realized by changing the size of the substrate according to the stretching factor S. Figure 3a shows the schematic diagram of the meta-lens change before stretching. The lateral distance between the PDMS substrate and the origin point is L, the thickness of the substrate is d, and the focal length is f. When the PDMS substrate is stretched along the x direction (as shown in Figure 3b), the stretched substrate lateral distance becomes L', the substrate thickness is d', and the focal length f is changed to f'. As the stretching range becomes larger, the length of the substrate becomes longer, the thickness becomes thinner, and the distance between the two unit cells becomes larger than before stretching. Considering that the focusing performance of the meta-lens becomes weaker when the stretching range becomes larger, here we only consider the change in the focal length when the stretching range is 100–120%.

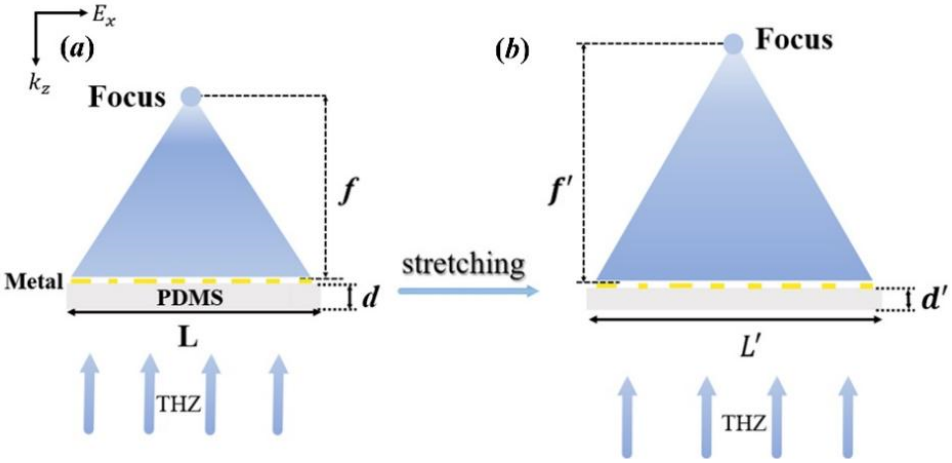

Figure 3. Schematic diagram of the change in the meta-lens before and after stretching. (**a**) Before substrate stretching; (**b**) after substrate stretching.

Firstly, the metasurface subwavelength unit cell structure forming the meta-lens is discussed. In order to reduce the computational complexity of the simulation process, the subwavelength period $p = 8\lambda/15$ is selected. The geometric dimensions of the metal unit cell structure are scanned by the electromagnetic finite time domain difference (FDTD) method, and the transmission coefficient and phase of the unit cell structure are obtained. In the simulation, terahertz waves are incident from the substrate along the *z*-axis. Periodic boundary conditions are selected in both the x and y directions, and in the z direction, the perfectly matched layers (PML) boundary conditions are used. By analyzing the scanning results obtained from the simulation, eight unit cell structures that can cover 0–2π phases are finally obtained, and the phase difference of the orthogonal polarization components of two adjacent antenna structures is $\pi/4$, as shown in Figure 4a. The transmission of the eight different unit cell structures that make up the meta-lens should be between 38% and 41%, and the detailed geometric parameters are illustrated in Table 1. Figure 4b shows the variation of the unit cell phase with the position before and after lateral stretching of the PDMS substrate. When the stretching amplitude of the substrate becomes larger, the phase change between the unit cell structures tends to decrease.

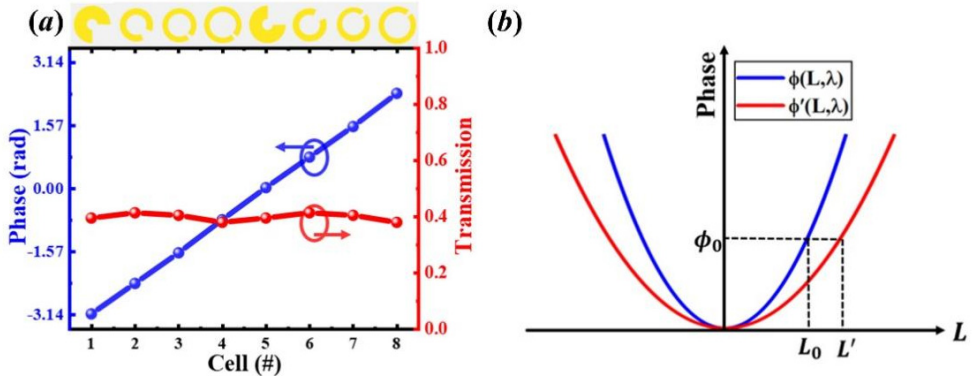

Figure 4. Phase response of the single-layer metal C-shaped SRRs. (**a**) Transmission coefficients and phase responses for eight discrete unit cell structures; (**b**) relationship between the lateral distance of PDMS substrate from the origin point and the phase before and after stretching.

Table 1. Design results of dynamically tunable meta-lens unit cell structure parameters of stretchable substrate single-layer metal structure.

Cell(#)								
Parameter	r_1=680μm r_2=200μm α= 88° θ= −45°	r_1=620μm r_2=380μm α= 45° θ= 45°	r_1=620μm r_2=420μm α= 15° θ= −45°	r_1=680μm r_2=480μm α= 12° θ= −45°	r_1=680μm r_2=200μm α= 88° θ= 45°	r_1=620μm r_2=380μm α= 45° θ= 45°	r_1=620μm r_2=420μm α= 15° θ= 45°	r_1=680μm r_2=480μm α= 12° θ= 45°
Phase(rad)	−3.12	−2.36	−1.60	−0.78	0.02	0.78	1.54	2.36
Transmission	0.39	0.41	0.40	0.38	0.39	0.40	0.41	0.38

3. Dynamically Focusing Analysis and Discussions

The focusing effects of the dynamically tunable meta-lens based on the stretchable substrate were then investigated with different stretching factors. To characterize the focusing efficiency of the designed meta-lens, the focusing efficiency is defined as the ratio of total electric field intensity in a circular aperture at the FWHM of focal spot to the total electric field intensity of incident light [29]. The overall diagram of the designed meta-lens is shown in Figure 2. The diameter and the numerical aperture of the meta-lens are 80 mm and 0.55, respectively. The initial focal length is designed to be 60 mm. Figure 5 depicts the electric distribution when the stretching factors of the PDMS substrate are 100%, 105%, 110%, 115%, and 120%, demonstrating that the focal length of the meta-lens becomes longer as the stretching amplitude increases. When the stretching factor increases from 100% to 120%, the focal length changes from 59.8 mm to 125.2 mm, and the dynamically focusing range can reach 109.4% of the minimum focal length. At the same time the focusing efficiency was changed from 5.5% to 10.5%. It can be seen that the electric field intensity gradually decreases with the increase in the stretching range, which is caused by the reduction in the phase difference between the metasurface unit cell structures as the stretching range increases.

Figure 6 shows the distribution of normalized electric field intensity corresponding to different stretching ranges of 100% to 120% at the frequency of 0.1 THz. As given in Figure 6a, when the stretching degree of the stretchable substrate increases, the focal length of the meta-lens gradually increases, which is agreed well with the results shown in Figure 5. Furthermore, the normalized electric field intensity exhibits an overall decreasing trend. The normalized electric field intensity reaches the maximum value when the stretching factor is 105%. The length of the focal point (in *z*-direction) becomes larger with the increase in the stretching factor. With the increase in the stretching factor, the PDMS

substrate gradually becomes thinner, which makes the focusing performance of the focal point decrease.

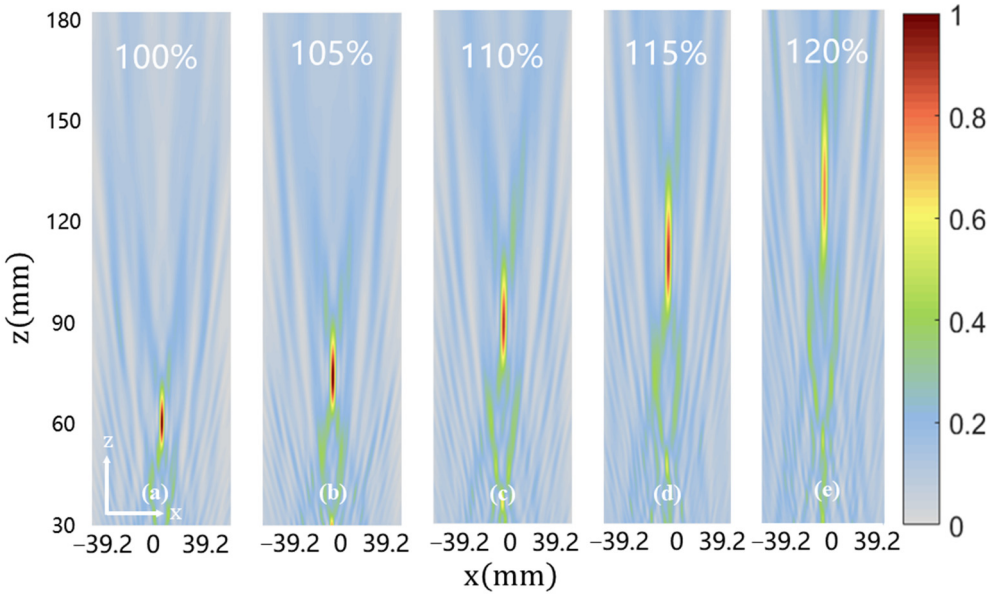

Figure 5. Normalized electric field distribution of the dynamically tunable meta-lens with different stretching factors.

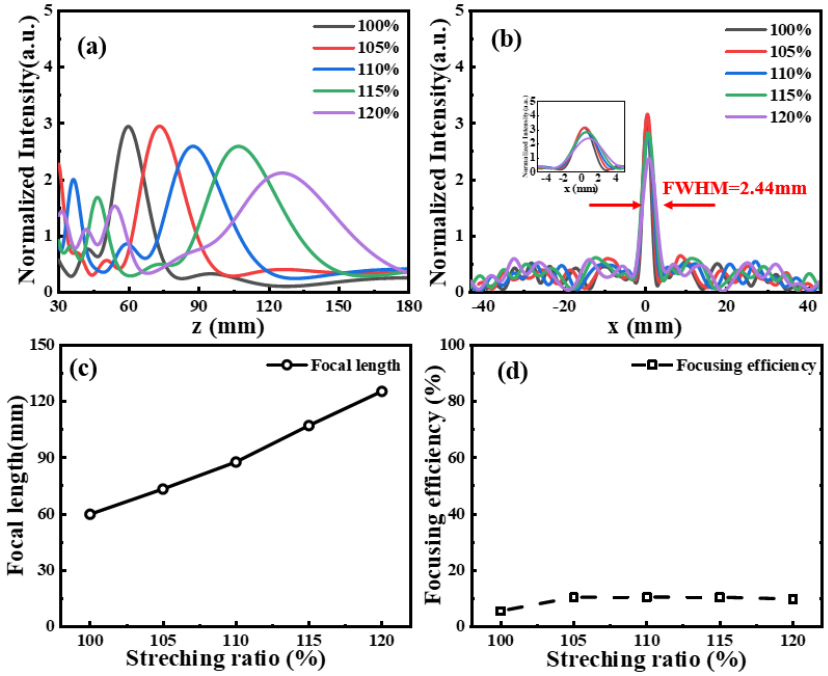

Figure 6. Dynamic focusing performance of single-layer metal C-shaped SRRs at the frequency of 0.1 THz. (**a**) Normalized electric field intensity distribution along the *z*-axis ($x = 0$) when the PDMS substrate is stretched from 100% to 120%; (**b**) normalized electric field intensity distribution in the focal plane when the PDMS substrate is stretched from 100% to 120%; (**c**) the change in the focal length with different stretching factors; (**d**) the change in the focusing efficiency with different stretching factors.

Figure 6b illustrates the electric field intensity distribution in the focal plane when the PDMS substrate is stretched from 100% to 120%. The width of the focal point (in *x* direction) tends to become larger when the stretching factor increases. The full width at half maximum

(FWHM) of the focal point is approximately 2.44 mm, which is 1.23 times the working wavelength. Figure 6c gives the change in focal length with different stretching factors, indicating a basically linear relationship between the focal length change and the stretching factor. Figure 6d shows the relationship between the focusing efficiency and the stretching factor. When the PDMS substrate is stretched from 100% to 120%, the focusing efficiency first increases and then decreases. The maximum focusing efficiency is approximately 10.5% for the stretching factor of 105%.

The performance comparison between the designed meta-lens structure and the previously reported structures are given in Table 2. It is observed that our meta-lens has a better focus tuning scope with less stretching magnitude.

Table 2. Performance comparison between the designed meta-lens and the previously reported structures with PDMS substrate.

Ref.	Cell Structure	Fabrication Realization	Stretching Scope	Wavelength/Band	Focusing Scope	Focusing Efficiency
[24]	Si	Yes	100–150%	915 nm	$2.3f_L$ (f_L = 600 μm)	75%
[22]	Au	Yes	100–130%	632 nm	$1.6f_L$ (f_L = 150 μm)	N/A
[30]	Al_2O_3	No	100–170%	660 nm	$2.2f_L$ (f_L = 42 μm)	N/A
This work	C-shaped SRR	No	100–120%	3 mm(0.1THz)	$2.2f_L$ (f_L = 60 mm)	10.5%

4. Conclusions

In this paper, a dynamically tunable meta-lens operating at the frequency of 0.1 THz is designed and investigated. Based on the principle of wavefront phase modulation, the phase change can reach 2π by treating the cross-polarized C-shaped metal split ring resonator structure. The dynamic focusing effects can be realized by stretching the PDMS substrate. In the investigation, when the length of the stretchable PDMS substrate changes from 100% to 120%, the focal length varies from 59.8 mm to 125.2 mm, and the focusing efficiency increases from 5.5% to 10.5%. In practical applications, the designed metasurface device has the advantages of simple fabrication and flexible modulation, exhibiting great potential in imaging systems.

Author Contributions: Conceptualization, X.L.; software and validation, X.H.; investigation, X.H. and H.L.; writing—original draft preparation, H.L.; writing—review and editing, D.Y.; funding acquisition, X.L. All authors have read and agreed to the published version of the manuscript.

Funding: This research was funded by National Key R&D Program of China (2021YFF0600300); Fundamental Research Funds for the Provincial Universities of Zhejiang (2021YW13); Basic Public Welfare Research Project of Zhejiang Province (No. TGN23C180006).

Institutional Review Board Statement: Not applicable.

Informed Consent Statement: Not applicable.

Data Availability Statement: Not applicable.

Conflicts of Interest: The authors declare no conflict of interest.

References

1. Yan, D.; Wang, Y.; Qiu, Y.; Feng, Q.; Li, X.; Li, J.; Qiu, G.; Li, J. A Review: The Functional Materials-Assisted Terahertz Met-amaterial Absorbers and Polarization Converters. *Photonics* **2022**, *9*, 335. [CrossRef]
2. Qiu, Y.; Yan, D.X.; Feng, Q.Y.; Li, X.J.; Zhang, L.; Qiu, G.H.; Li, J.N. Vanadium dioxide-assisted switchable multifunctional metamaterial structure. *Opt. Express* **2022**, *30*, 26544–26556. [CrossRef] [PubMed]
3. Yu, N.; Genevet, P.; Kats, M.A.; Aieta, F.; Tetienne, J.-P.; Capasso, F.; Gaburro, Z. Light Propagation with Phase Discontinuities: Generalized Laws of Reflection and Refraction. *Science* **2011**, *334*, 333–337. [CrossRef] [PubMed]
4. Lin, Y.; Jiang, C.P. Recent progress in tunable metalenses. *Chin. Opt.* **2020**, *13*, 43–61. (In Chinese) [CrossRef]

5. Sherrott, M.C.; Hon, P.W.C.; Fountaine, K.T.; Garcia, J.C.; Ponti, S.M.; Brar, V.W.; Sweatlock, L.A.; Atwater, H.A. Experimental Demonstration of >230° Phase Modulation in Gate-Tunable Graphene-Gold Reconfigurable Mid-Infrared Metasurfaces. *Nano Lett.* **2017**, *17*, 3027–3034. [CrossRef] [PubMed]
6. Belotelov, V.I.; Kreilkamp, L.E.; Akimov, I.A.; Kalish, A.N.; Bykov, D.A.; Kasture, S.; Yallapragada, V.J.; Venu Gopal, A.; Grishin, A.M.; Khartsev, S.I.; et al. Plasmon-mediated magneto-optical transparency. *Nat. Commun.* **2013**, *4*, 2128. [CrossRef]
7. Li, L.; Jun Cui, T.; Ji, W.; Liu, S.; Ding, J.; Wan, X.; Bo Li, Y.; Jiang, M.; Qiu, C.W.; Zhang, S. Electromagnetic reprogrammable coding-metasurface holograms. *Nat. Commun.* **2017**, *8*, 197. [CrossRef]
8. Liu, P.X.; Zhao, Y.; Qin, R.X.; Mo, S.G.; Chen, G.X.; Gu, L.; Chevrier, D.M.; Zhang, P.; Guo, Q.; Zang, D.D.; et al. Photochemical route for synthesizing atomically dispersed palladium catalysts. *Science* **2016**, *352*, 797–800. [CrossRef]
9. Koch, U.; Hoessbacher, C.; Emboras, A.; Leuthold, J. Optical memristive switches. *J. Electroceramics* **2017**, *39*, 239–250. [CrossRef]
10. She, A.; Zhang, S.Y.; Shian, S.; Clarke, D.R.; Capasso, F. Adaptive metalenses with simultaneous electrical control of focal length, astigmatism, and shift. *Sci. Adv.* **2018**, *4*, eaap9957. [CrossRef]
11. Jiang, L.; Wang, Y.; Wang, X.; Ning, F.; Wen, S.; Zhou, Y.; Chen, S.; Betts, A.; Jerrams, S.; Zhou, F.L. Electrohydrodynamic printing of a dielectric elastomer actuator and its application in tunable lenses. *Compos. Part A Appl. Sci. Manuf.* **2021**, *147*, 106461. [CrossRef]
12. Kang, L.; Jenkins, R.P.; Werner, D.H. Recent progress in active optical metasurfaces. *Adv. Opt. Mater.* **2019**, *7*, 1801813. [CrossRef]
13. Arbabi, E.; Arbabi, A.; Kamali, S.M.; Horie, Y.; Faraji-Dana, M.S.; Faraon, A. MEMS-tunable dielectric metasurface lens. *Nat. Commun.* **2018**, *9*, 812. [CrossRef]
14. Han, Z.; Colburn, S.; Majumdar, A.; Böhringer, K.F. MEMS-actuated metasurface Alvarez lens. *Microsyst. Nanoeng.* **2020**, *6*, 79. [CrossRef]
15. Balli, F.; Sultan, M.A.; Hastings, J.T. Rotationally tunable varifocal 3D metalens. *Opt. Lett.* **2021**, *46*, 3548–3551. [CrossRef]
16. Zhu, W.M.; Song, Q.H.; Yan, L.B.; Zhang, W.; Wu, P.C.; Chin, L.K.; Cai, H.; Tsai, D.P.; Shen, Z.X.; Deng, T.W.; et al. A flat lens with tunable phase gradient by using random access reconfigurable metamaterial. *Adv. Mater.* **2015**, *27*, 4739–4743. [CrossRef]
17. Pishvar, M.; Harne, R.L. Foundations for soft, smart matter by active mechanical metamaterials. *Adv. Sci.* **2020**, *7*, 2001384. [CrossRef]
18. Kowerdziej, R.; Olifierczuk, M.; Salski, B.; Parka, J. Tunable negative index metamaterial employing in-plane switching mode at terahertz frequencies. *Liq. Cry.* **2012**, *39*, 827–831. [CrossRef]
19. Ferraro, A.; Zografopoulos, D.C.; Caputo, R.; Beccherelli, R. Periodical elements as low-cost building blocks for tunable terahertz filters. *IEEE Photon. Technol. Lett.* **2016**, *28*, 2459–2462. [CrossRef]
20. Yan, L.B.; Zhu, W.M.; Wu, P.C. Adaptable metasurface for dynamic anomalous reflection. *Appl. Phys. Lett.* **2017**, *110*, 20. [CrossRef]
21. Dong, L.; Zhang, B.; Duan, J.; Yang, H.; Liu, Y.; Xu, Y.; Xu, H.; Chen, B. Conformal transparent metamaterials inducing ultra-broadband absorption and polarization conversion. *J. Infrared Millim. Terahertz Waves* **2019**, *40*, 905–916. [CrossRef]
22. Ee, H.S.; Agarwal, R. Tunable metasurface and flat optical zoom lens on a stretchable substrate. *Nano Lett.* **2016**, *16*, 2818–2823. [CrossRef] [PubMed]
23. Callewaert, F.; Velev, V.; Jiang, S.; Sahakian, A.V.; Kumar, P.; Aydin, K. Inverse-designed stretchable metalens with tunable focal distance. *Appl. Phys. Lett.* **2018**, *112*, 091102. [CrossRef]
24. Kamali, S.M.; Arbabi, E.; Arbabi, A.; Horie, Y.; Faraon, A. Highly tunable elastic dielectric metasurface lenses. *Laser Photonics Rev.* **2016**, *10*, 1002–1008. [CrossRef]
25. Li, X.J.; Hou, X.M.; Cheng, G.; Qiu, G.H.; Yan, D.X.; Li, J.S. Simulation on tunable graphene metasurface focusing mirror based on flexible substrate. *Chin. Opt.* **2021**, *14*, 1019–1028. (In Chinese)
26. Sathukarn, A.; Jia, Y.C.; Boonruang, S.; Horprathum, M.; Tantiwanichapan, K.; Prasertsuk, K.; Thanapirom, C.; Kusolthossakul, W.; Kasamsook, K. The Simulation of a Surface Plasmon Resonance Metallic Grating for Maximizing THz Sensitivity in Refractive Index Sensor Application. *Int. J. Opt.* **2020**, *2020*, 3138725. [CrossRef]
27. Yang, Y.; Duan, S.; Zhao, H. Advances in constructing silver nanowire-based conductive pathways for flexible and stretchable electronics. *Nanoscale* **2022**, *14*, 11484–11511. [CrossRef] [PubMed]
28. Yu, N.F.; Capasso, F. Flat Optics with Designer Metasurfaces. *Nat. Mater.* **2014**, *13*, 139–150. [CrossRef]
29. Arbabi, A.; Horie, Y.; Ball, A.J.; Bagheri, M.; Faraon, A. Subwavelength-thick lenses with high numerical apertures and large efficiency based on high-contrast transmit arrays. *Nat. Commun.* **2015**, *6*, 7069–7074. [CrossRef]
30. Lin, P.; Lin, Y.S.; Lin, J.; Yang, B.R. Stretchable metalens with tunable focal length and achromatic characteristics. *Results Phys.* **2021**, *31*, 105005. [CrossRef]